Contents of this file

Introduction

This supplementary material shows forced model response for all models studied (**Fig. S1**); the forced model response for each individual region and subregion for all GCMs (**Fig. S2**); and per-month distribution of large eruptions at two volcanoes (**Fig. S3**). Details of models used are given in **Tab. S1**. Data were processed as described in the main text.

To retrieve the data shown in **Figure S3**, the Global Volcanism Program database (Global Volcanism Program 2013) was filtered to include only "Confirmed" and "Observed" historical eruptions at Reventador and Vesuvius with a Maximum Explosivity Index of 3 or greater. As an additional filter, only eruptions with a "Start Date Day Uncertainty" of ≤ 5 were included, resulting in 10 eruptions at Reventador and 26 eruptions at Vesuvius. Full details may be found in the accompanying code.

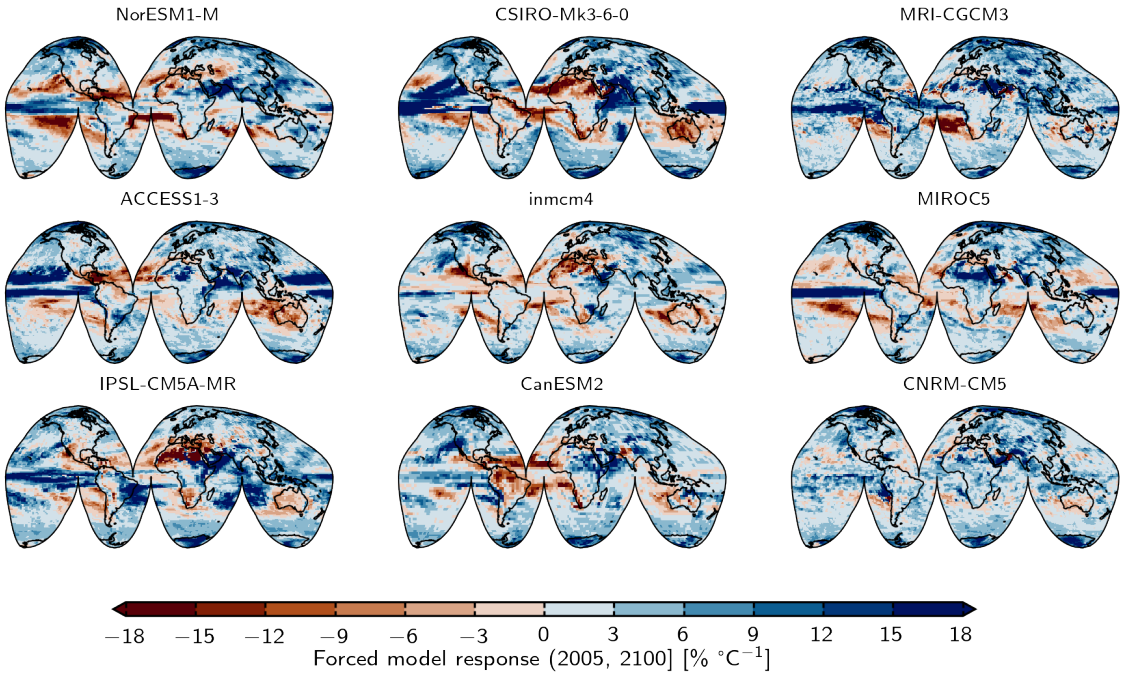

Figure S1. Forced model response for all compared models. GCM codes (as listed in Table 1, Methods) are shown above the corresponding map. Forced model response (FMR) as ***RX*** versus $\langle \boldsymbol{T} \rangle$ over the timeframe from 2005 or 2006 to 2100, normalized to 2006. Blue tones represent an increase in extreme rainfall with increased global warming, red tones represent a decrease.

Regions

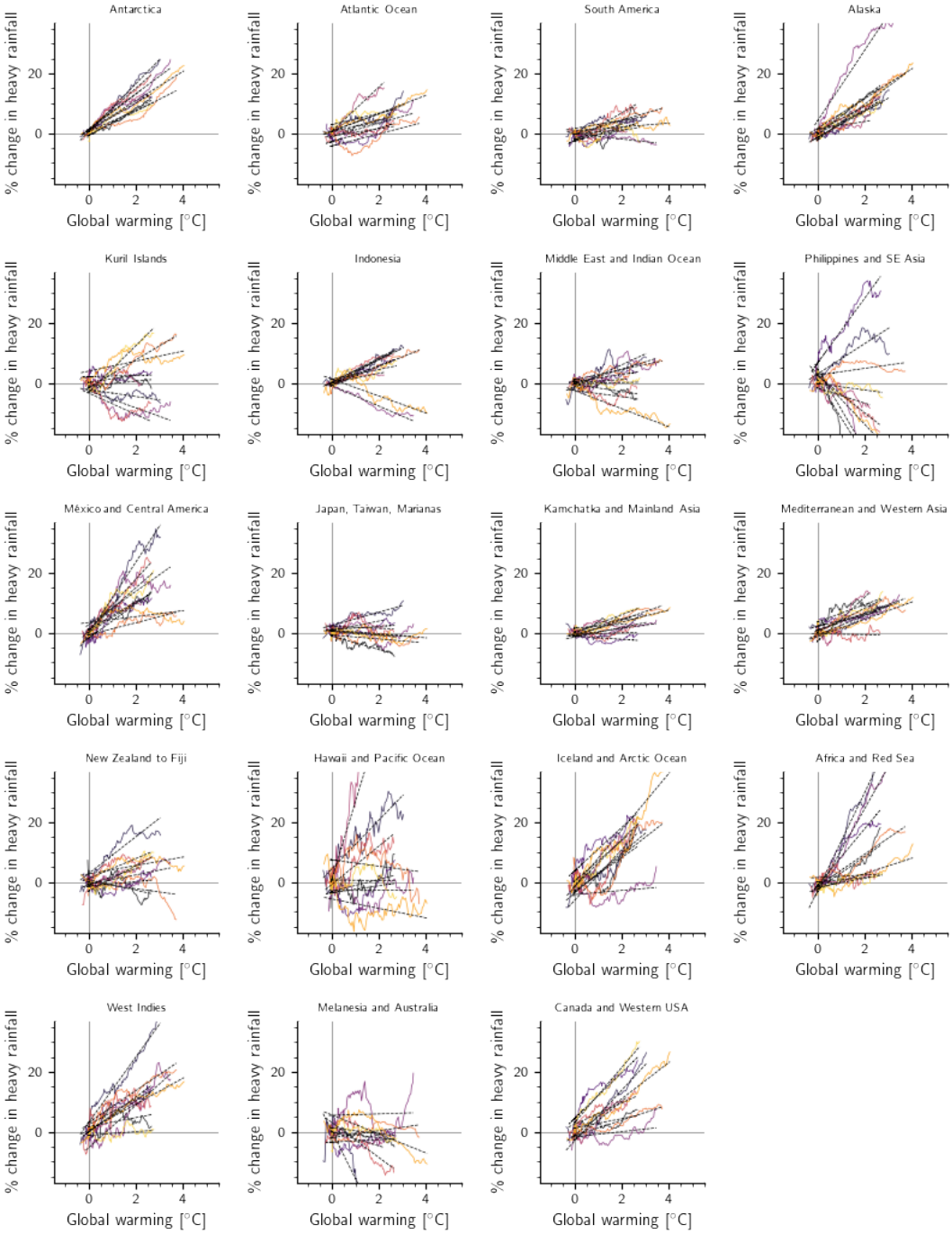

Subregions

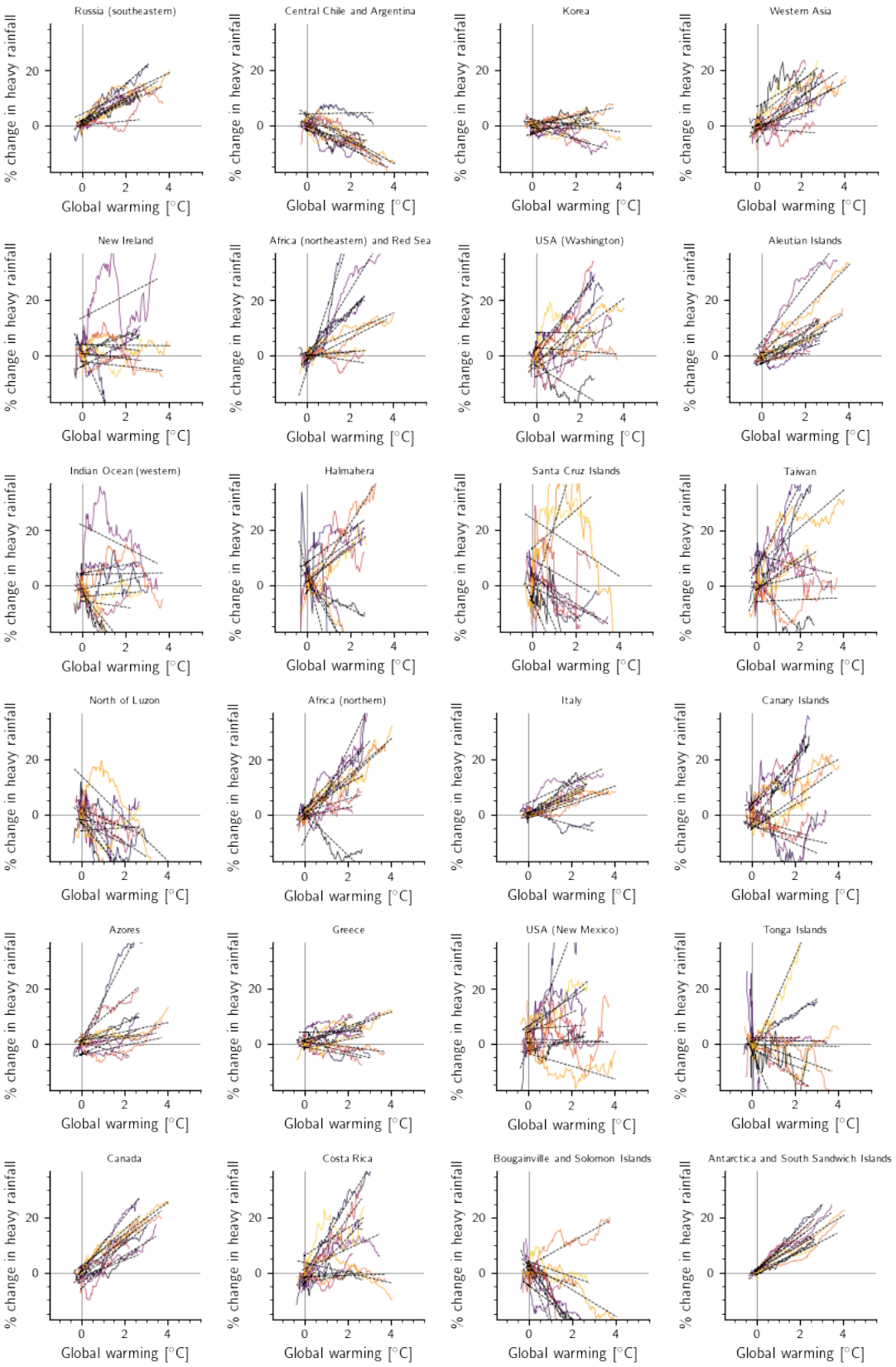
Russia (southeastern)
Central Chile and Argentina
Korea
Western Asia
New Ireland
Africa (northeastern) and Red Sea
USA (Washington)
Aleutian Islands
Indian Ocean (western)
Halmahera
Santa Cruz Islands
Taiwan
North of Luzon
Africa (northern)
Italy
Canary Islands
Azores
Greece
USA (New Mexico)
Tonga Islands
Canada
Costa Rica
Bougainville and Solomon Islands
Antarctica and South Sandwich Islands
% change in heavy rainfall
Global warming [°C]
0
20
0
2
4

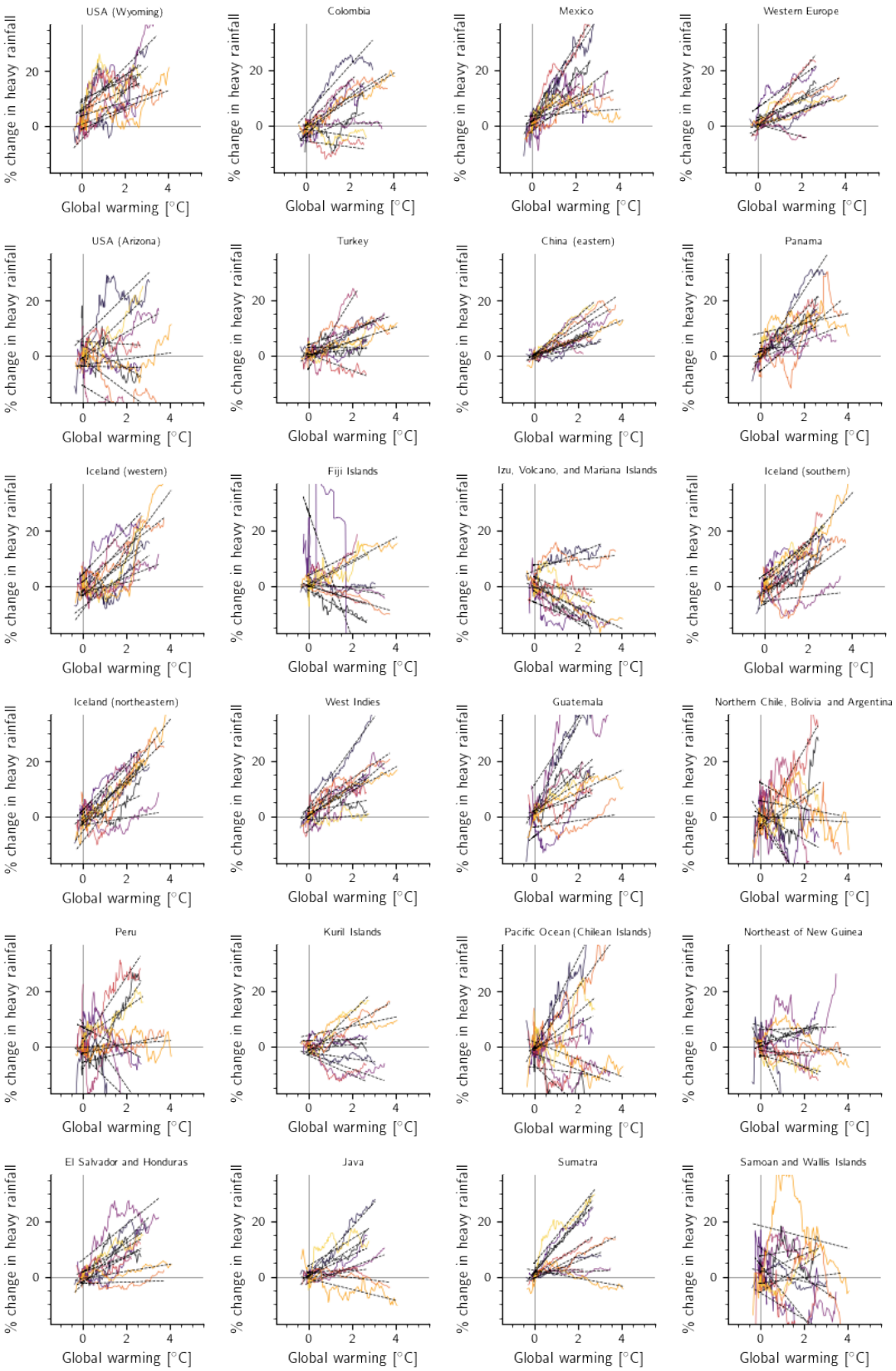
USA (Wyoming)
Colombia
Mexico
Western Europe
USA (Arizona)
Turkey
China (eastern)
Panama
Iceland (western)
Fiji Islands
Izu, Volcano, and Mariana Islands
Iceland (southern)
Iceland (northeastern)
West Indies
Guatemala
Northern Chile, Bolivia and Argentina
Peru
Kuril Islands
Pacific Ocean (Chilean Islands)
Northeast of New Guinea
El Salvador and Honduras
Java
Sumatra
Samoan and Wallis Islands
% change in heavy rainfall
Global warming [°C]
0
20
0
2
4

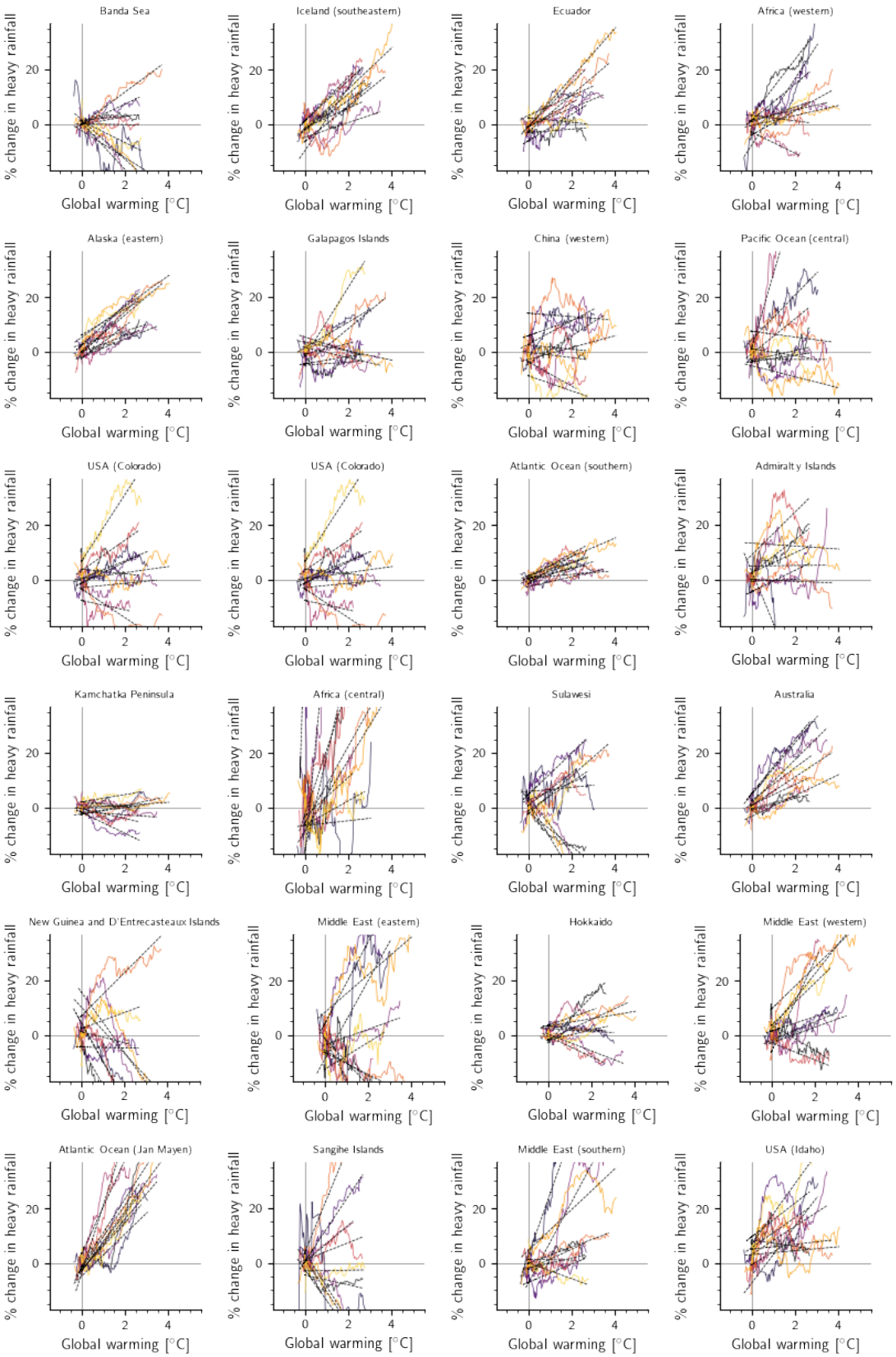
Banda Sea
Iceland (southeastern)
Ecuador
Africa (western)
Alaska (eastern)
Galapagos Islands
China (western)
Pacific Ocean (central)
USA (Colorado)
USA (Colorado)
Atlantic Ocean (southern)
Admiralty Islands
Kamchatka Peninsula
Africa (central)
Sulawesi
Australia
New Guinea and D'Entrecasteaux Islands
Middle East (eastern)
Hokkaido
Middle East (western)
Atlantic Ocean (Jan Mayen)
Sangihe Islands
Middle East (southern)
USA (Idaho)
% change in heavy rainfall
Global warming [°C]
0
20
0
2
4

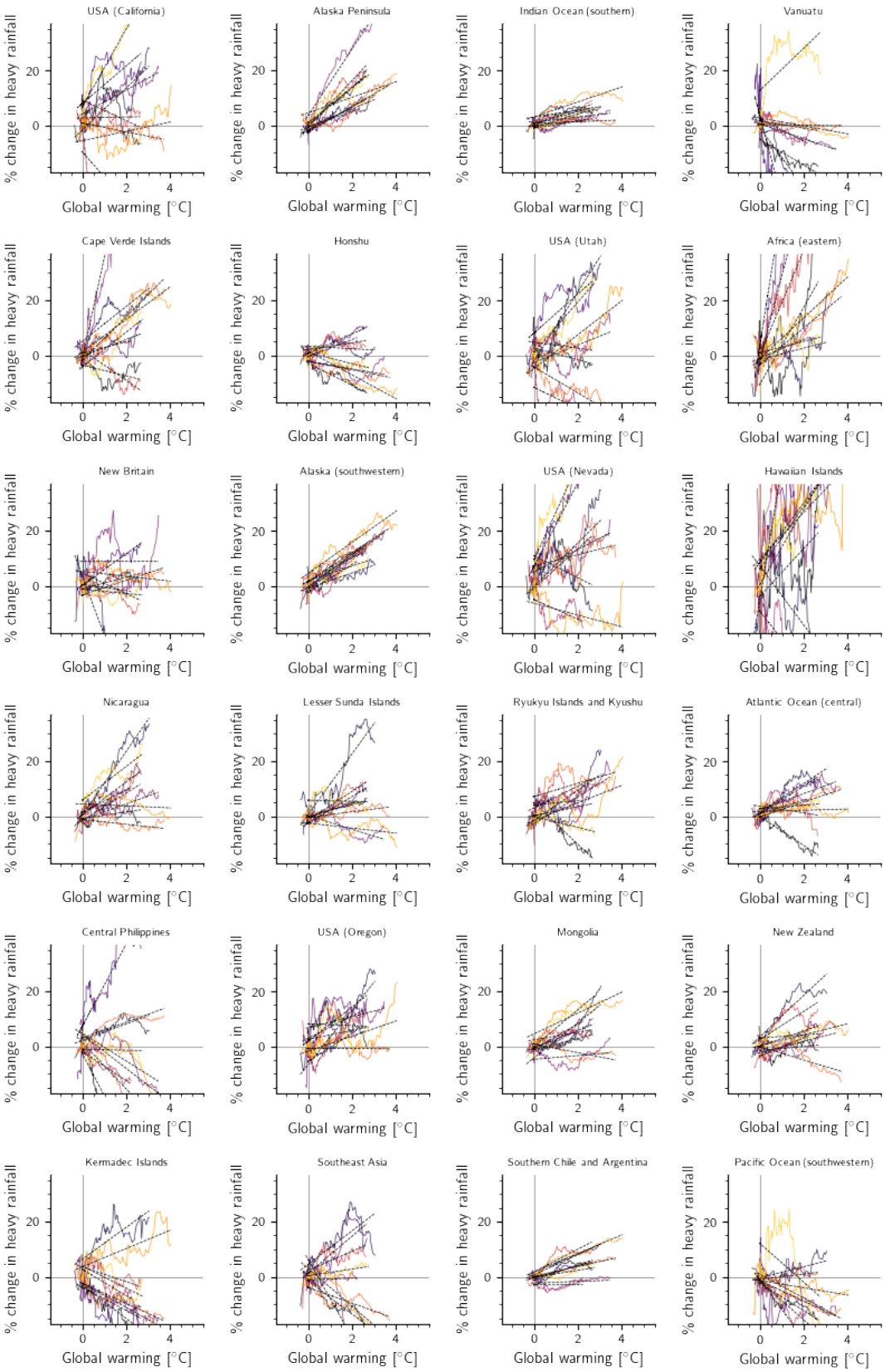
USA (California)
Alaska Peninsula
Indian Ocean (southern)
Vanuatu
Cape Verde Islands
Honshu
USA (Utah)
Africa (eastern)
New Britain
Alaska (southwestern)
USA (Nevada)
Hawaiian Islands
Nicaragua
Lesser Sunda Islands
Ryukyu Islands and Kyushu
Atlantic Ocean (central)
Central Philippines
USA (Oregon)
Mongolia
New Zealand
Kermadec Islands
Southeast Asia
Southern Chile and Argentina
Pacific Ocean (southwestern)
% change in heavy rainfall
Global warming [°C]
0
20
0
2
4

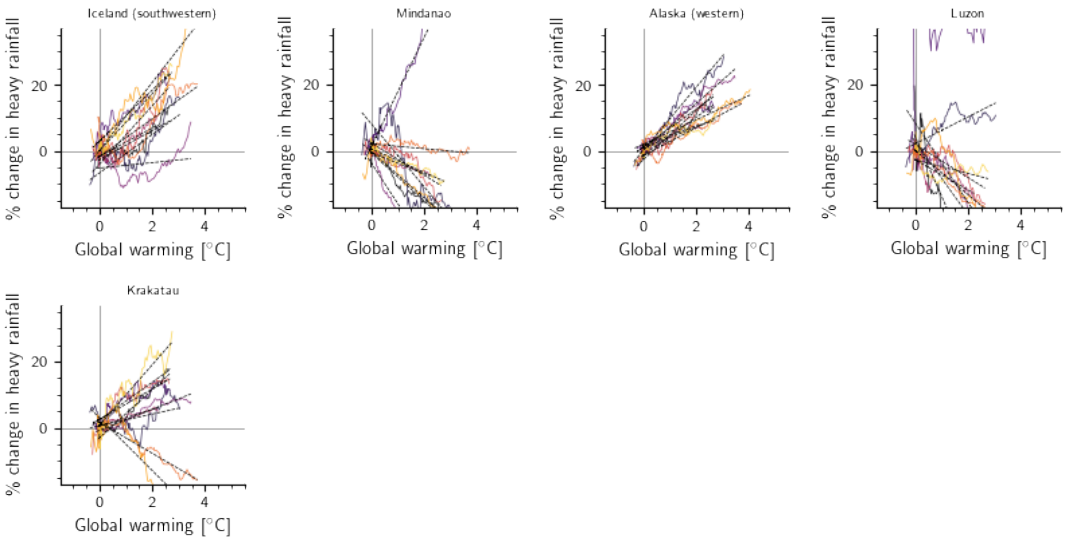

Figure S2. Forced model responses at different spatial scales. Percent change in modelled heavy rainfall per degree of global warming, from nine climate models: ACCESS1.3, CNRM-CM5, CSIRO-Mk3.6.0, CanESM2, INM-CM4, IPSL-CM5A-MR, MIROC5, MRI-CGCM3, and NorESM1-M. Data are shown as a 30-yr rolling mean, normalized to January 2021. Dashed black lines are linear regression of response for each model. Data are areal averages, calculated by including model grids that contain a Holocene-active volcano for each of the Global Volcanism Program's defined "Region" and "Subregion" categories (19 and 101 categories, respectively).

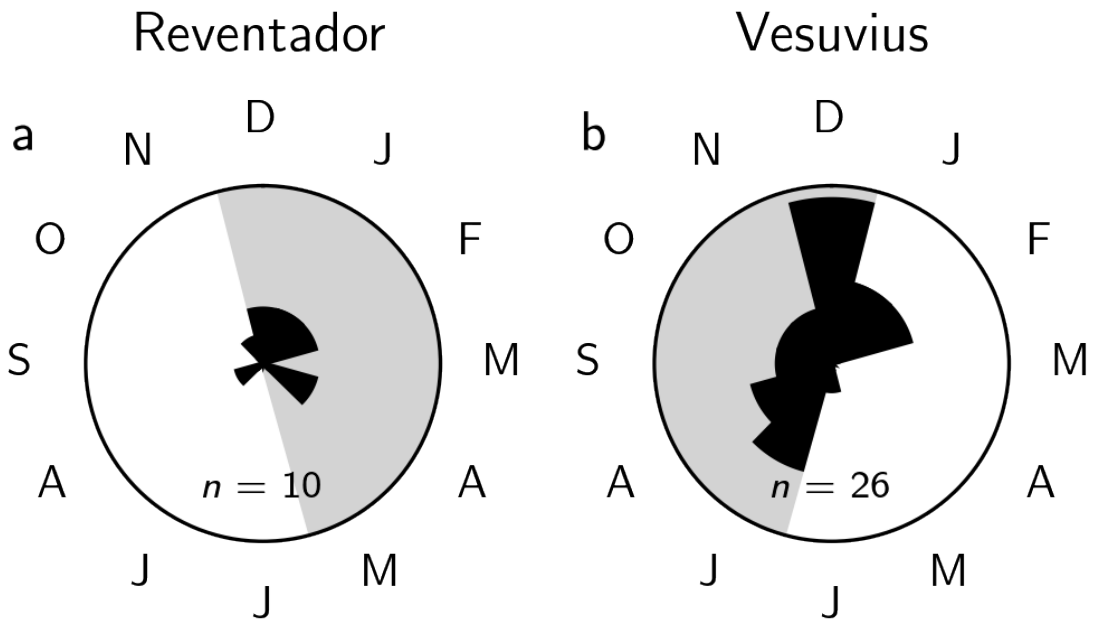

Figure S3. Distribution of eruptions ≥VEI 3 for **a** Reventador (Ecuador), and **b** Vesuvius (Italy). In both panels, the labels [J, F, …, D], correspond to months of the year, and each bar reflects the number of historical eruptions in the GVP database occurring within that month. The total number ***n*** reflects the number of eruptions in the filtered dataset. Grey shaded region indicates the period of the year receiving the most rainfall.

Table S1. Nine CMIP5 models used in this study, including their spatial resolutions. Data accessed via Earth System Grid Federation servers, in particular the node hosted by the Lawrence Livermore National Laboratory: https://esgf-node.llnl.gov/search/cmip5/.

Model	Modelling center	Spatial resolution	
		Nodes	Degrees (lat × lon)
ACCESS1.3	CSIRO (Commonwealth Scientific and Industrial Research Organisation, Australia), and BOM (Bureau of Meteorology, Australia)	145 × 192	1.25 × 1.875
CNRM-CM5	Centre National de Recherches Météorologiques/Centre Européen de Recherche et Formation Avancées en Calcul Scientifique	128 × 256	1.4008 × 1.40625
CSIRO-Mk3.6.0	CSIRO (Commonwealth Scientific and Industrial Research Organisation, Australia), and BOM (Bureau of Meteorology, Australia)	96 × 192	1.8653 × 1.875
CanESM2	Canadian Centre for Climate Modelling and Analysis	64 × 128	2.7906 × 2.8125
INM-CM4	Institute for Numerical Mathematics, Russia	120 × 180	1.5 × 2
IPSL-CM5A-MR	Institut Pierre-Simon Laplace, France	96 × 96	1.2676 × 2.5
MIROC5	Atmosphere and Ocean Research Institute (The University of Tokyo), National Institute for Environmental Studies, and Japan Agency for Marine-Earth Science and Technology, Japan	128 × 256	1.4008 × 1.40625
MRI-CGCM3	Meteorological Research Institute, Japan	160 × 320	1.12148 × 1.125
NorESM1-M	Norwegian Climate Centre, Norway	96 × 144	1.8947 × 2.5